Downregulation of cyclin-dependent kinase inhibitors p21 and p27 in pressure-overload hypertrophy

JIAN-MEI LI AND GAVIN BROOKS
Cardiovascular Cellular and Molecular Biology, Cardiovascular Research, The Rayne Institute, St. Thomas' Hospital, London SE1 7EH, United Kingdom

Li, Jian-Mei, and Gavin Brooks. Downregulation of cyclin-dependent kinase inhibitors p21 and p27 in pressure-overload hypertrophy. *Am. J. Physiol.* 273 (*Heart Circ. Physiol.* 42): H1358–H1367, 1997.—We postulated that the cyclin-dependent kinase inhibitors p21 and p27 could regulate the alterations in growth potential of cardiomyocytes during left ventricular hypertrophy (LVH). LVH was induced in adult rat hearts by aortic constriction (AC) and was monitored at *days 0, 1, 3, 7, 14, 21,* and *42* postoperation. Relative to sham-operated controls (SH), left ventricle (LV) weight-to-body weight ratio in AC increased progressively with time without significant differences in body weight or right ventricle weight-to-body weight ratio. Atrial natriuretic factor mRNA increased significantly in AC to 287% at *day 42* compared with SH ($P < 0.05$), whereas p21 and p27 mRNA expression in AC rats decreased significantly by 58% ($P < 0.03$) and 40% ($P < 0.05$) at *day 7*, respectively. p21 and p27 protein expression decreased significantly from *days 3* to *21* in AC versus SH, concomitant with LV adaptive growth. Immunocytochemistry showed p21 and p27 expression in cardiomyocyte nuclei. Thus downregulation of p21 and p27 may modulate the adaptive growth of cardiomyocytes during pressure overload-induced LVH.

cardiomyocytes; cell cycle; left ventricular hypertrophy; rat

LEFT VENTRICULAR hypertrophy (LVH) due to chronic hemodynamic overload or myocardial injury is one of the most important compensatory responses of the heart. Although this process is initially compensatory, there can be a pathological transition in which the myocardium becomes dysfunctional (9, 29). Mammalian adult cardiomyocytes are terminally differentiated cells that have been permanently withdrawn from the cell cycle (reviewed in Ref. 18). However, chronic stimulation of cardiomyocytes, e.g., from hypertension or increased cardiac workload, results in growth of myocytes by hypertrophy rather than any increase in myocyte cell number. Previous studies have demonstrated that LVH is not a sole adaptive response to an increased workload because other biological changes play an important role in this process (1, 6, 7, 14) such as alterations in gene expression, including induction of the expression of immediate early genes (e.g., c-*myc* and c-*fos*), embryonic genes [e.g., atrial natriuretic factor (ANF)], and other genes (e.g., transforming growth factor-β) that regulate cell growth and differentiation. However, the signaling molecules that mediate the growth of cardiomyocytes during LVH remain unknown.

Cell cycle regulation involves the expression of cyclins and the activation of their associated cyclin-dependent kinases (CDKs) (18). The various cyclin-CDK complexes undergo changes in their constitutive components that drive cells from one stage of the cell cycle to another (19, 22). In addition to this positive regulation of the cell cycle, negative controls on cell cycle progression also are exerted such that a number of CDK inhibitors (CDKIs) specifically bind to and inhibit the activity of cyclin-CDK complexes, thereby causing cells to arrest in the cell cycle. Two such CDKIs, p21 (also known as CIP1/WAF1/SDI1) (8, 11, 21) and p27 (KIP1) (24, 27), have been shown to play important roles in arresting many cell types during the G_0 and G_1/S phases of the cell cycle (18, 21, 27). p21 also directly inhibits DNA synthesis by blocking proliferating cell nuclear antigen binding to DNA polymerase-δ (28). Because the molecular and cellular phenomena observed during LVH (i.e., activation of embryonic gene transcription, increase in mRNA synthesis, protein content, and cell size) are predominantly G_1 phase changes (20, 22), we postulated that CDKIs, such as p21 and p27, may play a role in the alterations in growth potential of cardiomyocytes during hypertrophy. In the present study, we produced pressure overload-induced LVH in rats and examined the mRNA and protein expression of p21 and p27 in left ventricle (LV) tissues by reverse transcriptase (RT)-polymerase chain reaction (PCR) and immunoblotting, respectively, at different time points after operation. In addition, we investigated the molecular localization of p21 and p27 in cardiomyocytes by immunocytochemistry. Our results suggest, for the first time, that certain CDKIs, such as p21 and p27, may modulate the adaptive growth of cardiomyocytes during pressure overload-induced LVH in rats.

MATERIALS AND METHODS

Materials. [α-^{32}P]dCTP redivue (3,000 Ci/mmol) and enhanced chemiluminescence Western blotting reagents were purchased from Amersham International. Oligo(dT) cellulose beads, proteinase K, and bovine serum albumin (BSA) type V were purchased from Sigma. Rabbit polyclonal antibodies against p21 and p27, corresponding peptides for competition studies, and goat anti-rabbit immunoglobulin G (IgG) horseradish peroxidase-conjugated antibody were purchased from Santa Cruz Biotechnology. All other chemicals used were of the highest grade available commercially.

Cell culture. Murine NIH/3T3 fibroblasts were cultured in Dulbecco's modified Eagle's medium (DMEM) containing 10% fetal calf serum (GIBCO-BRL, Paisley, Scotland). Cultures were growth arrested by maintaining cells in DMEM-Waymouth's medium (2:1) for 48 h before use. All cultures were kept in a humidified atmosphere containing 95% O_2-5% CO_2 at 37°C.

Animals. Adult male Wistar rats (starting weight, 166 ± 3 g) were obtained from Banton and Kingman (Hull, UK). Animals were killed by an approved method in accordance

with the UK Home Office Animals (Scientific Procedures) Act (1986).

Induction of LVH and cardiac tissue preparation. Chronic pressure overload was produced in rats by subtotal suprarenal constriction of the abdominal aorta (AC) as described previously (16). Briefly, under anesthesia with 0.3 ml/kg Hypnorm and 2.5 mg/kg diazepam intraperitoneally, the aorta was carefully exposed through an abdominal incision. A uniform degree (0.45 mm diameter) of constriction was achieved by fixing a titanium clip around the aorta (16). Age-matched sham-operated rats (SH) underwent the same operation but without AC. Both AC and SH rats were housed and fed under identical conditions. Six rats from each group were killed at *days 1*, *3*, *7*, *14*, *21*, and *42* after surgery. In addition, six rats that did not undergo any operation were used as *day 0* controls. Body weight was recorded for each rat, both on the day of operation and on the day of death when the heart was excised and weighed. The atria were carefully dissected from the ventricles, and LV tissue was separated from right ventricle (RV) tissue and was weighed. Each sample of LV tissue was split into three portions and was used for mRNA extraction, protein preparation, and immunohistochemistry, respectively. Heart tissue was frozen immediately in liquid N_2 until required for analysis.

mRNA preparation and RT-PCR. Poly-A^+ enriched RNA from LV tissue of AC and SH rats was prepared according to the method of Brooks et al. (4). Briefly, tissue was ground finely in liquid N_2 and was homogenized using a Ystral X10/25 homogenizer (Scientific Instruments Centre) in lysis buffer (50 mg/ml) containing 0.2 M NaCl, 0.2 M tris(hydroxymethyl)aminomethane (Tris)·HCl, 0.15 M $MgCl_2$, 2% sodium dodecyl sulfate (SDS), and 200 μg/ml proteinase K at pH 7.5. After proteinase K digestion overnight at 45°C, the lysate was adjusted to a final concentration of 0.3 M NaCl. mRNA was obtained by binding to oligo(dT) cellulose beads (2 mg/ml). Beads were washed extensively with binding buffer (0.5 M NaCl and 0.01 M Tris·HCl, pH 7.5), and mRNA was eluted from the beads with 2 × 200 μl of 0.01 M Tris·HCl (pH 7.5). mRNA was precipitated with 1/10 vol of 3 M NaOAc and 2 vol of absolute ethanol and was resuspended in 50 μl of double-distilled water. Purified mRNA (0.3 μg) from each LV sample was reverse transcribed using a cDNA RT-PCR kit (Promega, Madison, WI) as recommended by the manufacturer. After ethanol precipitation, the cDNA samples were dissolved in 50 μl ribonuclease (RNase)-free water. One microliter of this diluted cDNA was diluted further to 4 μl with RNase-free water, and 1 μl of each was used for PCR amplification of glyceraldehyde-3-phosphate dehydrogenase (GAPDH), ANF, p21, and p27. At this dilution and using 30 PCR cycles, [^{32}P]dCTP-labeled time course experiments showed that the products of GAPDH, ANF, p21, and p27 amplification were all within the linear phase of the reaction under the conditions used (Fig. 1 and Table 1). Indeed, similar conditions have been used successfully by our group for semiquantitative analysis of gene expression, including GAPDH and ANF, in rat ventricular tissue (12). PCR was performed using the aforesaid 1 μl of diluted cDNA in a total volume of 50 μl containing 50 μM *N*-2-hydroxyethylpiperazine-*N*′-2-ethanesulfonic acid (pH 7.9), 1.5 mM $MgCl_2$, 100 μM of each dNTP, 2.5 U *Taq* polymerase (GIBCO-BRL), and 100 pmol each of sense and antisense primers. Primers were directed against the mouse sequences for p21 (sense, 5′-GTTGTCTCTTCGGTCCCGTG-3′; antisense 5′-CGCAGATTGGTCTTCTGCAAG-3′) (30) and for p27 (sense 5′-GCCTGGAGCGGATGGACGC-3′; antisense 5′-CTGTGGAGCAGACGCCCAAGAAG-3′) (27). Primers for GAPDH (sense 5′-CCTTCATTGACCTCAAC-3′; antisense 5′-AGTTGTCATGGATGACC-3′) were used for each sample as an internal control for mRNA integrity and equal loading. Primers for rat ANF (sense 5′-ATGGGCTCCTTCTCCATCAC-3′; antisense 5′-TCTTCGGTACCGGGAAGCTG-3′), which have been reported to be overexpressed in LVH (2), also were used for each sample as a positive control for the induction of hypertrophy. PCRs were carried out for GAPDH, ANF, and p21 as follows: 1 cycle of 94°C for 1 min, then 30 cycles of 94°C for 45 s, 63°C for 45 s, 72°C for 90 s plus 1 cycle of 72°C for 2 min. PCR for p27 used identical conditions except the annealing temperature was 69°C. PCR products were analyzed on 1.5% agarose gels. To compare the levels of mRNA expression between AC and SH LV tissues, 1 μCi of [α-^{32}P]dCTP (3,000 Ci/mmol) was added to each PCR reaction cocktail, and PCRs were carried out using the same condi-

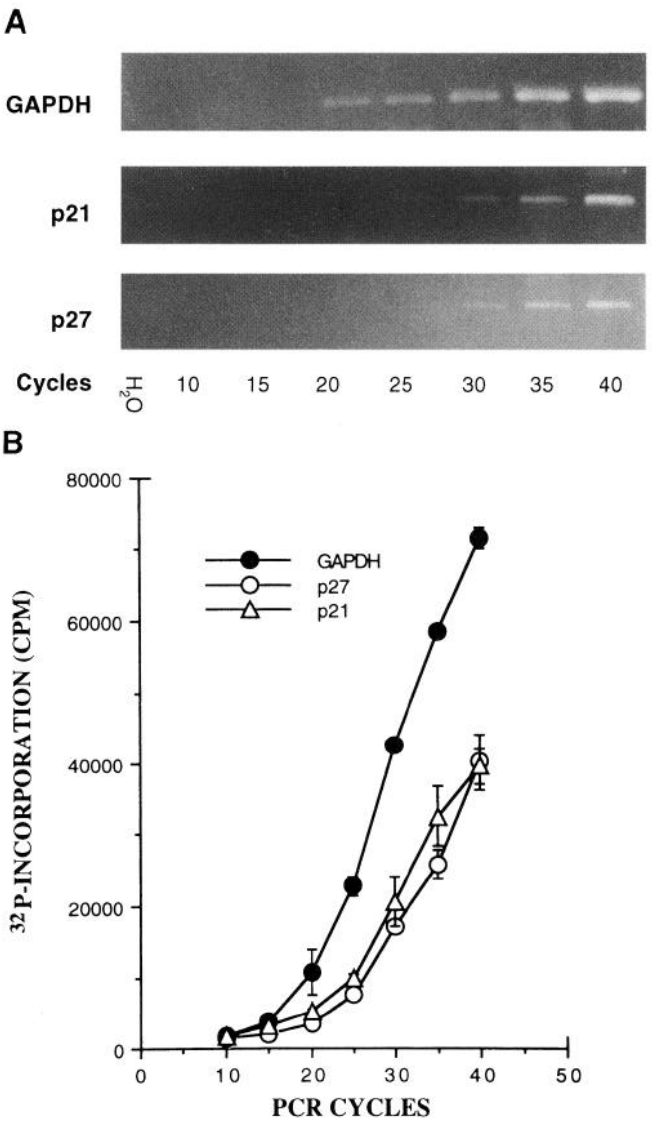

Fig. 1. *A*: ethidium bromide-stained gel showing levels of reaction products obtained using 0.25 μg reverse transcriptase (RT) product and after various cycles of polymerase chain reaction (PCR) amplification for glyceraldehyde-3-phosphate dehydrogenase (GAPDH), p21, and p27 in untreated adult rat left ventricle (LV) tissue using the conditions described in MATERIALS AND METHODS. *B*: graph demonstrating linearity of reaction products obtained using 0.25 μg RT product and after various cycles of [^{32}P]dCTP-labeled PCR amplification for GAPDH, p21, and p27 in untreated adult rat LV tissue using the conditions described in MATERIALS AND METHODS. CPM, counts per minute.

Table 1. *Demonstration of linearity of PCR conditions using different concentrations of RT product and 30 cycles of amplification*

RT Product, μl	GAPDH	p21	p27
0.05	223.0 ± 36.0	0	0
0.10	417.3 ± 54.9	141.8 ± 9.7	80.5 ± 12.9
0.25	858.5 ± 48.9	460.0 ± 31.2	234.3 ± 1.3
0.50	1272.0 + 104.7	820.3 + 54.5	677.0 + 28.7

Values are means ± SE of densitometric indexes obtained from 2 separate experiments. Purified mRNA (0.3 μg) was obtained from untreated adult rat left ventricle (LV) tissue and was used for the reverse transcriptase (RT) reaction. Different amounts (in μl) of RT product were dissolved in 50 μl of distilled water, and polymerase chain reaction (PCR) was carried out for 30 cycles as described in MATERIALS AND METHODS. Resultant agarose gels were scanned twice densitometrically and were analyzed using NIH Image. Accordingly, 0.25 μl was selected as the experimental concentration for all subsequent analyses. GAPDH, glyceraldehyde-3-phosphate dehydrogenase.

tions as described above. After separation on 1.5% agarose gels, ethidium bromide-stained bands were excised under ultraviolet (UV) light, and the radioactivity incorporated into PCR products was detected by β-scintillation counting. All samples were tested in duplicate, and at least three different mRNA samples were investigated at each time point after operation from both AC and SH rats. Levels of radioactivity incorporated into the p21, p27, or ANF PCR products were normalized by comparison with the levels of radioactivity incorporated into the GAPDH product from the same sample.

Protein extraction and immunoblotting. Tissue (200 mg/ml) was homogenized using a Ystral C10/25 homogenizer in an ice-cold extraction buffer containing 0.05 M Tris, 0.15 M NaCl, 2 mM EDTA, 2 mM phenylmethylsulfonyl fluoride, 2 μg/ml leupeptin, and 2 μg/ml aprotinin (pH 7.4). After sonication, Triton X-100 was added to a final concentration of 0.5%. The lysate was extracted on ice for 15 min and was centrifuged at 12,000 *g* for 20 min. Protein concentrations in each preparation were determined according to the method of Bradford (3) using BSA as a standard. Immunoblotting was performed as described previously (4). Briefly, proteins (40 μg) were separated on 15% SDS-polyacrylamide gels and were transferred to nitrocellulose membranes. Membranes were blocked with 5% nonfat milk in phosphate-buffered saline-0.2% Tween 20 (PBST), followed by incubation with rabbit polyclonal antibodies to p21 or p27 diluted (1:1,000) in PBST containing 1% nonfat milk for 1 h at room temperature. After being washed with PBST, membranes were incubated with goat anti-rabbit IgG conjugated to horseradish peroxidase for 30 min at room temperature. Bands were visualized by enhanced chemiluminescence and were quantified using densitometry. Each protein sample was analyzed twice, and at least three different samples from AC and SH rats were examined at each time point after operation.

Immunocytochemistry. LV tissues from AC and SH rats at *days 0, 7, 14,* and *21* postoperation were snap frozen and were cryosectioned into 6-μm sequential sections. Pretreatment of sections and immunofluorescence was carried out as previously described (17) using rabbit polyclonal antibodies against cardiac troponin I (a gift from Dr. P. Cummins, University of Birmingham, UK), p21, or p27 (5 μg/ml). Normal rabbit IgG (5 μg/ml) was used in each experiment as a negative control. For competitive inhibition assays, antibodies to p21 and p27 were preincubated for 30 min at room temperature with 1 μg/ml of synthesized peptide for p21 and p27, respectively, before incubation with sections. Primary antibodies were incubated with the relevant section for 30 min at room temperature, and the specific antibody binding was detected using either biotin-conjugated goat anti-rabbit IgG followed by streptavidin-Texas Red (Amersham) or fluorescein isothiocyanate (FITC)-conjugated goat anti-rabbit IgG (Sigma). Specific fluorescent staining of cardiac tissue was identified under UV light with an Olympus BH2-RFCA microscope using an oil-immersion lens (magnification ×40) and was photographed using Kodak film. The number of nuclei positively stained with antibodies to p21 or p27 were counted within the microscopic field and were compared with the total number of nuclei stained on the same section and, within the same microscopic field, with 1.5 μg/ml propidium iodide. Three sections from each tissue were analyzed by two independent assessors, and three different tissues were used for each time point after operation.

Statistical analysis. Results are presented as means ± SE and were obtained from three different mRNA or protein

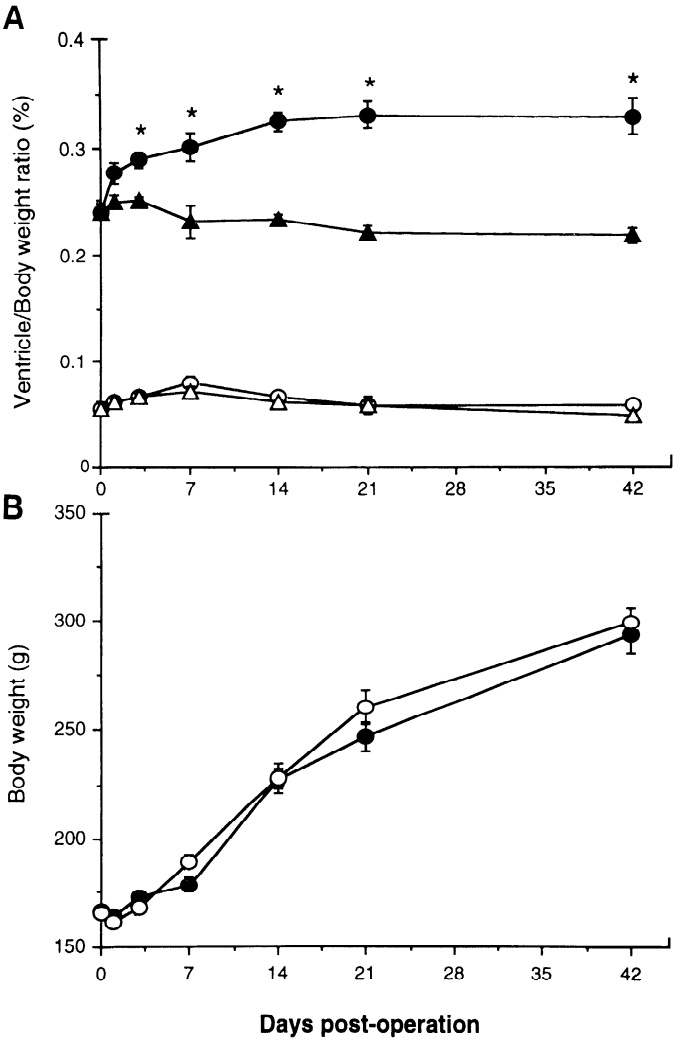

Fig. 2. Effect of aortic constriction (AC) on ventricular weight (*A*) and body weight (*B*). Hearts from 6 separate rats from each treatment group [AC and sham-operated controls (SH)] were obtained at *days 0, 1, 3, 14, 21,* and *42* after operation and were separated into LV and right ventricle (RV) tissues. *A*: ●, LV weight-to-body weight ratio from AC rats; ▲, LV weight-to-body weight ratio from SH rats; ○, RV weight-to-body weight ratio from AC rats; △, RV weight-to-body weight ratio from SH rats. *B*: ●, body weight from AC rats; ○, body weight from SH rats. Results are expressed as means ± SE. *$P <$ 0.01 compared with time-matched SH rats.

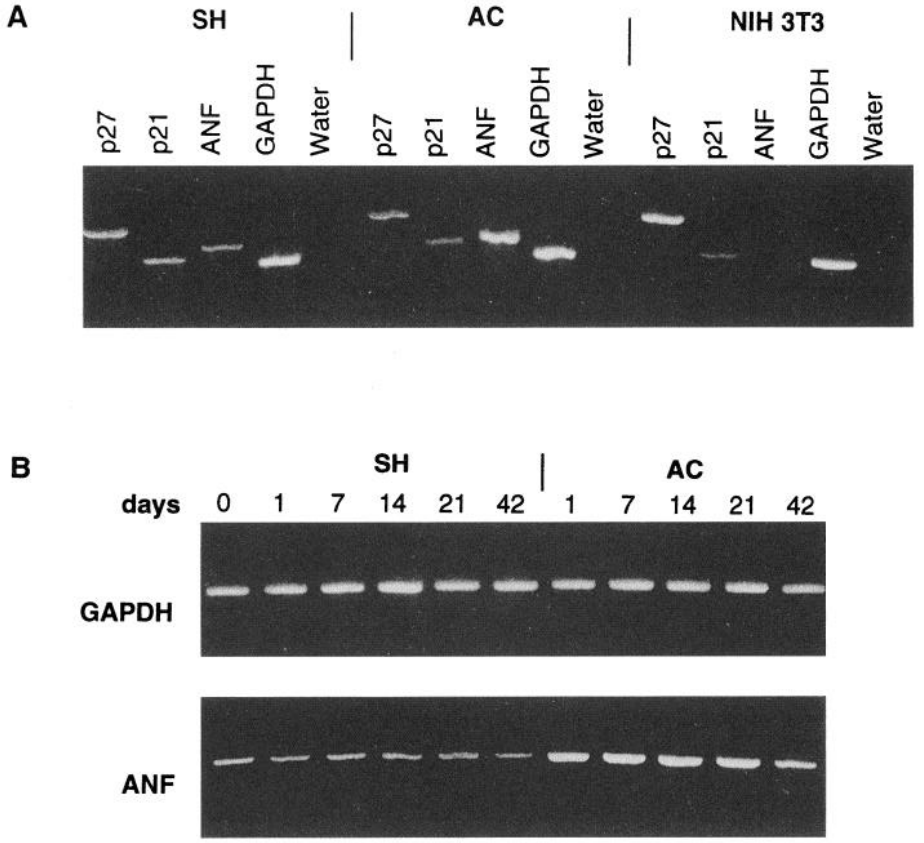

Fig. 3. Detection of GAPDH, atrial natriuretic factor (ANF), p21, and p27 mRNA in LV tissue of rats by reverse transcription (RT)-PCR. Agarose gels (1.5%) were stained with ethidium bromide and were visualized under ultraviolet light. *A*: expression of GAPDH, ANF, p21, and p27 mRNA in LV tissue obtained from rats at *day 7* postoperation and in NIH/3T3 fibroblasts. *B*: time course for mRNA expression of GAPDH and ANF in LV tissue obtained from AC and SH rats.

samples at each time point, each of which was analyzed in duplicate. Means were analyzed by one-way analysis of variance, and, if a significant difference was observed, then each AC value was compared with the SH value at the same time point using the Bonferroni *t*-test. Values where $P < 0.05$ were considered significant.

RESULTS

Effect of AC on ventricular mass. Six rats from either AC or SH groups were killed at *days 1*, *3*, *7*, *14*, *21*, and *42* after surgery. Body weight and ventricular weight were measured, and results were expressed as the ratio of ventricular weight to body weight. Relative to age-matched SH controls, LV weight-to-body weight ratio in AC rats increased progressively with time (e.g., by 11% at *day 1*, 30% at *day 7*, 39% at *day 14*, and 50% at *day 21*; $P < 0.001$; Fig. 2*A*). However, no significant difference was observed in total body weight (Fig. 2*B*) or in RV weight-to-body weight ratio after operation between AC and SH rats (Fig. 2*A*). After 21 days, LV mass in AC rats reached a plateau, with no further increase in LV weight observed up to 6 wk after operation.

Expression of GAPDH, ANF, p21, and p27 mRNAs after AC and SH operation. After the demonstration of linear RT-PCR conditions at 30 cycles for GAPDH, p21, and p27 (Fig. 1 and Table 1), the detection of GAPDH, ANF, p21, and p27 transcripts by RT-PCR was determined in LV tissue obtained from both AC and SH rats at *day 7* postoperation. A representative ethidium bromide-stained agarose gel containing the separated PCR fragments for GAPDH, ANF, p21, and p27 is shown in Fig. 3*A*. In addition, mRNA from the mouse NIH/3T3 fibroblast cell line, which has been shown in our laboratory to express p21 and p27 48 h after serum starvation, was used as a positive control for each RT-PCR reaction. Both p21 and p27 mRNAs were expressed in NIH/3T3 fibroblasts and in LV tissues both from AC and SH rats and exhibited single bands of 415 and 535 base pairs, respectively. Expression of ANF mRNA was detected at high levels in LV tissue from AC rats compared with levels expressed in SH rat LV tissue at all time points after operation (Fig. 3, *A* and *B*) and was maintained at these elevated levels for the duration of the experiment. As expected, ANF mRNA was undetectable in NIH/3T3 cells (Fig. 3*A*). In contrast, GAPDH mRNA expression showed little oscillation throughout the postoperative time course and no significant difference was observed between AC and SH rats (Fig. 3*B*), thereby confirming the use of GAPDH as a suitable internal control for normalization of results between samples. To compare the levels of expression of ANF, p21, and p27 mRNAs at different time points after AC or SH operation, RT-PCR reactions were carried out in the presence of [α-^{32}P]dCTP, and the degree of incorporated radioactivity was detected by β-scintillation counting. All results were normalized to the expression of the GAPDH gene at each time point after operation and were expressed as a ratio to GAPDH. Consistent with previous reports (e.g., Ref. 2), ANF mRNA expression was significantly increased in all AC rats as early as *day 1* until *day 42* after operation

compared with SH controls (Fig. 4*A*; $P < 0.05$). In contrast, the expression of p21 (Fig. 4*B*) and p27 (Fig. 4*C*) mRNAs were downregulated significantly in AC rat LV tissue compared with time-matched SH control animals such that a 45% decrease was observed at *day 3* and a 58% decrease at *day 7* postoperation for p21 ($P < 0.03$) and a 36% decrease at *day 3* and a 40% decrease at *day 7* postoperation for p27 ($P < 0.05$). By *day 14* postoperation, the levels of p21 and p27 mRNA in AC rats returned to the levels observed in SH controls.

Changes in p21 and p27 protein expression after AC and SH operation. To determine the expression of p21 and p27 proteins during LVH, we measured the amount of p21 and p27 proteins in LV tissues from AC and SH rats by immunoblotting. Equal protein loading in each experiment was confirmed by Coomassie blue staining of the gels and by probing a duplicate transfer membrane with a rabbit polyclonal antibody to cardiac troponin I. Each experiment was repeated twice to confirm the reproducibility of the results. A representative experiment is shown in Fig. 5. Thus the amount of p21 protein detected in LV tissue obtained from AC rats decreased gradually with time, whereas LV tissue obtained from SH rats showed a constant level of p21 protein throughout the *day 1-42* postoperative period. Interestingly, the levels of p27 protein in LV tissues from both AC and SH rats increased progressively with age, such that rats at *day 42* postoperation expressed more p27 protein than rats at earlier time points after operation. However, the levels of p27 protein were significantly lower from *days 1* to *14* after operation in AC rats compared with SH rats. Between *days 21* and *42* of operation, p27 protein in AC rats increased dramatically, such that no significant difference was observed between the levels of p27 protein in AC and SH operated rats at *day 42*. Figure 5 also shows that the reduction in p21 and p27 protein expression in AC rats was not due to variations in the amount of protein loaded as duplicate gels probed with an antibody to troponin I showed a band at 28 kDa, for which the level altered very little in samples from both AC and SH controls throughout the 6-wk postoperative period. The specificity of antibody binding was confirmed in each case by competitive inhibition with synthetic peptides for p21 and p27 (0.8 μg/ml), which abolished specifically the bands at 21 and 27 kDa, respectively (data not shown). The changes in expression of p21 and p27 protein following AC and SH operation were quantified by densitometric scanning of autoradiographs obtained from three separate hearts with two determinations per tissue sample. Results were normalized individually to the density of the troponin I immunoreactive band for each sample, and the results were expressed as the ratio of p21 to troponin I or p27 to troponin I expression (Fig. 6). A significant reduction in p21 protein expression in LV tissue from AC rats was observed from *days 3* to *21* after operation compared with SH rats ($P < 0.03$; Fig. 6*A*). Similarly, p27 protein expression was reduced significantly in LV tissues from

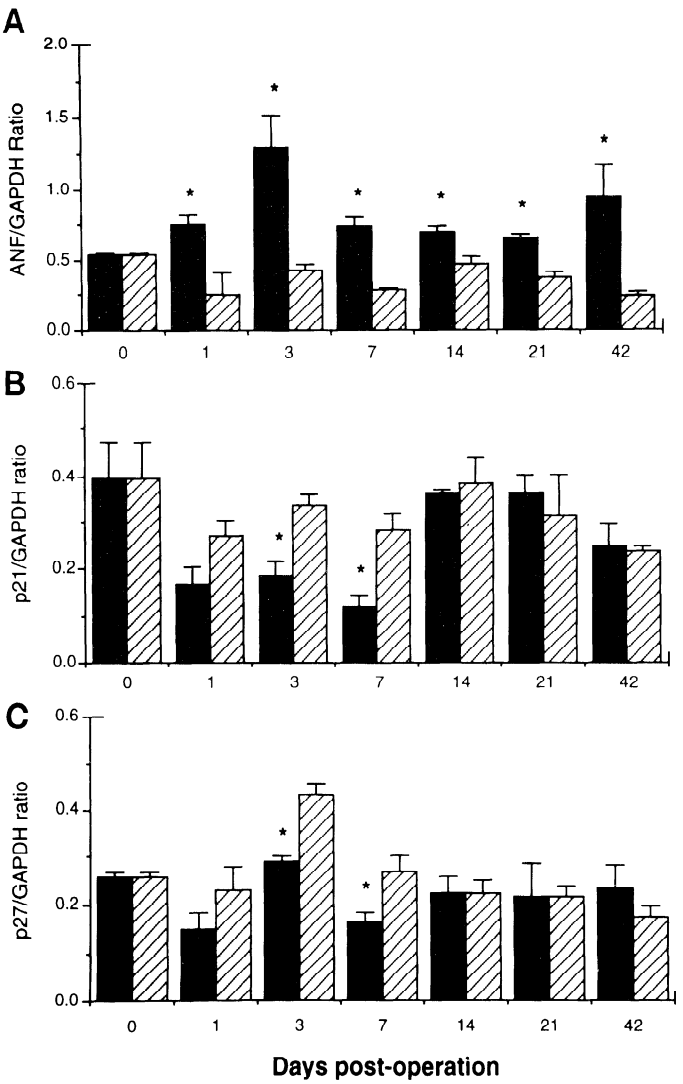

Fig. 4. Graph to show the changes in mRNA expression of ANF (*A*), p21 (*B*), and p27 (*C*) after AC and SH operation detected by [α-^{32}P]dCTP-labeled RT-PCR. Filled bars, AC rats; hatched bars, SH rats. Results were normalized individually to the GAPDH mRNA expression detected in every sample and are expressed as a ratio to GAPDH. Levels of mRNA in AC animals at any time point were compared with SH controls obtained at the same time point. Results are means ± SE obtained from 3 separate hearts and 2 determinations per heart. *$P < 0.05$ compared with time-matched SH rats.

AC rats compared with SH controls from *days 1* to *21* after operation ($P < 0.05$; Fig. 6*B*).

Immunocytochemical detection of p21 and p27 in cardiomyocytes. To determine whether p21 and p27 were expressed in cardiomyocytes, we performed immunofluorescent staining on cardiac cryosections from the same series of LV tissues as used for mRNA and protein measurements. An antibody to cardiac troponin I was used to demonstrate the presence of cardiomyocytes and specifically stained the cytoplasm, but not the nuclei, of cardiomyocytes and showed a typical rod cell-shaped morphology on longitudinal sections (Fig. 7, *A*, *C*, and *D*). In addition, the antibody to cardiac troponin I demonstrated that, under the same magnification, a significant increase in myocyte cell size occurred in AC rat hearts 14 days after operation (Fig.

7*D*) compared with SH controls (Fig. 7*C*). When the same sections were double stained with the antibody to p27, we demonstrated very clearly the nuclear localization of p27 in cardiomyocytes from LV tissues of both SH (Fig. 7*C*) and AC (Fig. 7*D*) rats. Specificity of p27 antibody binding to the nuclei of myocardial cells was demonstrated by competition studies with the synthetic p27 peptide (1 μg/ml; compare Fig. 7*E* with Fig. 7*B*). Thus it can be seen clearly that competition with peptide results in a low level of background immunofluorescence consistent with abolition of specific p27 nuclear staining (Fig. 7*B*) compared with staining with p27 antibody alone (Fig. 7*E*). To calculate the number of nuclei positively stained by the p27 antibody, sections from both SH and AC rats were double stained with antibodies to p27 and propidium iodide. At *day 14* postoperation, the antibody for p27 positively stained 15–25% of nuclei on LV sections obtained from AC rats (Fig. 7, *E* and *F*), whereas ~80% of nuclei were positively stained with this antibody on LV sections obtained from SH rats at the same postoperative period (data not shown). Thus the in situ study confirmed the reduction of p27 protein in LV tissue observed by immunoblotting during the development of pressure overload-induced LVH. Furthermore, these results showed that this response occurs in cardiomyocytes. p21 staining of cardiomyocyte nuclei on a transverse section obtained from an untreated adult rat heart on *day 0* is shown in Fig. 8*A*. Incubation of sequential sections from the same LV with a rabbit polyclonal antibody to laminin, which is a major component of the cardiomyocyte membrane (23, 26), outlined cardiomyocytes (Fig. 8*B*) and demonstrated characteristic myocyte T tubules (Fig. 8, *C* and *E*). Using a triple-staining approach with propidium iodide (to identify nuclei), antibodies to laminin (to stain myocyte membranes) and p21, we demonstrated very clearly the downregulation of p21 in the nuclei of cardiomyocytes from AC rats (Fig. 8, *E* and *F*) compared with SH controls (Fig. 8, *C* and *D*) obtained 14 days after operation. The antibody to p21 positively stained >90% of nuclei in cardiomyocytes on LV sections from SH rats 14 days after operation (Fig. 8*C*), whereas this antibody stained <10% of nuclei in cardiomyocytes on LV sections from AC rats after the same postoperative period (Fig. 8*E*). Thus the immunocytochemical results correlated very well with the mRNA and protein expression data obtained from AC and SH rats and demonstrated the downregulation of both p21 and p27 in cardiomyocytes during the development of LVH.

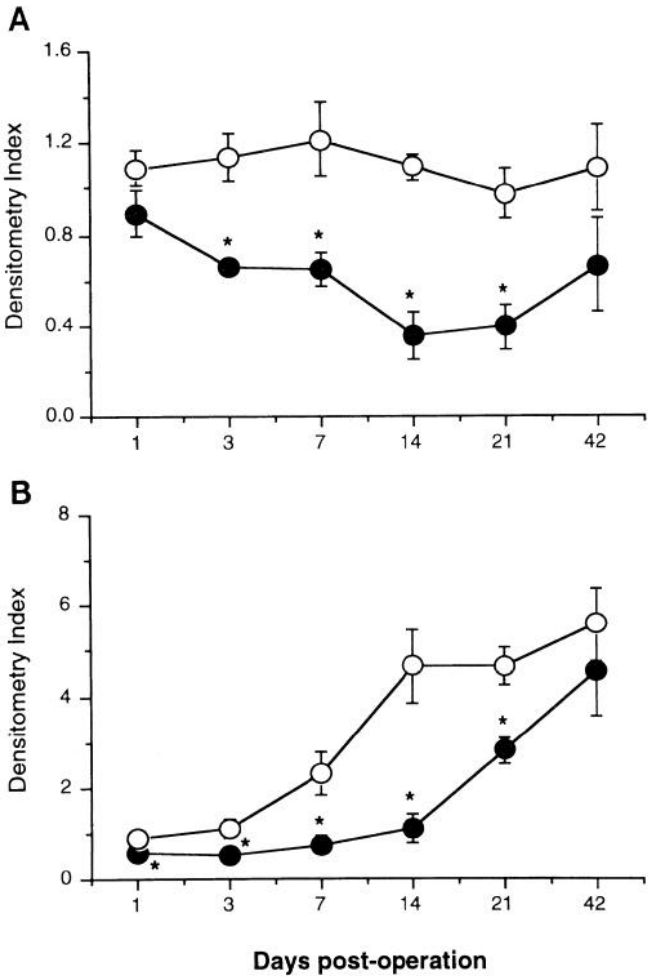

Fig. 6. Graph to show results from densitometric scans of immunoblots for p21 (*A*) and p27 (*B*) protein expression. ●, AC group; ○, SH group. Three different protein samples from each group at each time point after operation were examined. Results were normalized to the expression of troponin I protein per sample and are expressed as a ratio of p21 to troponin I (*A*) or p27 to troponin I (*B*). Results are means ± SE. $^*P < 0.05$ compared with time-matched SH rats.

DISCUSSION

In this study we report, for the first time, the expression and subcellular localization of two negative modulators of the cell cycle, the CDKIs p21 and p27,

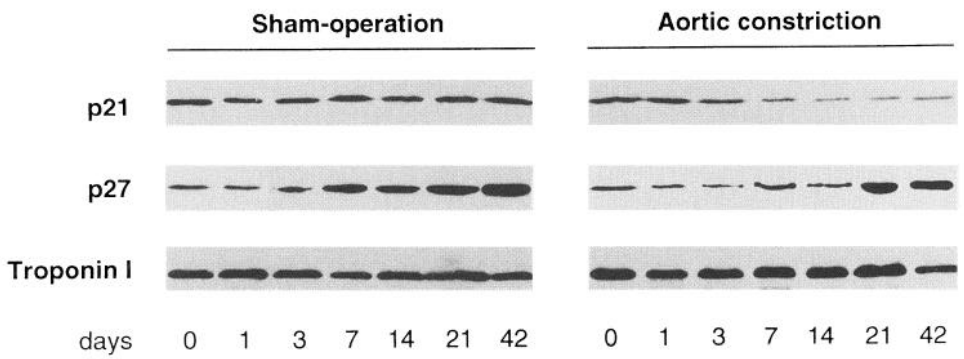

Fig. 5. Immunoblot analysis to show the expression of p21 and p27 proteins in LV tissue obtained from rats after AC and SH operation. Equal amounts of protein (40 μg) from each sample were separated by 15% SDS-polyacrylamide gel electrophoresis and were transferred to nitrocellulose. Filters were probed with antibodies to p21, p27, and cardiac troponin I as described in MATERIALS AND METHODS.

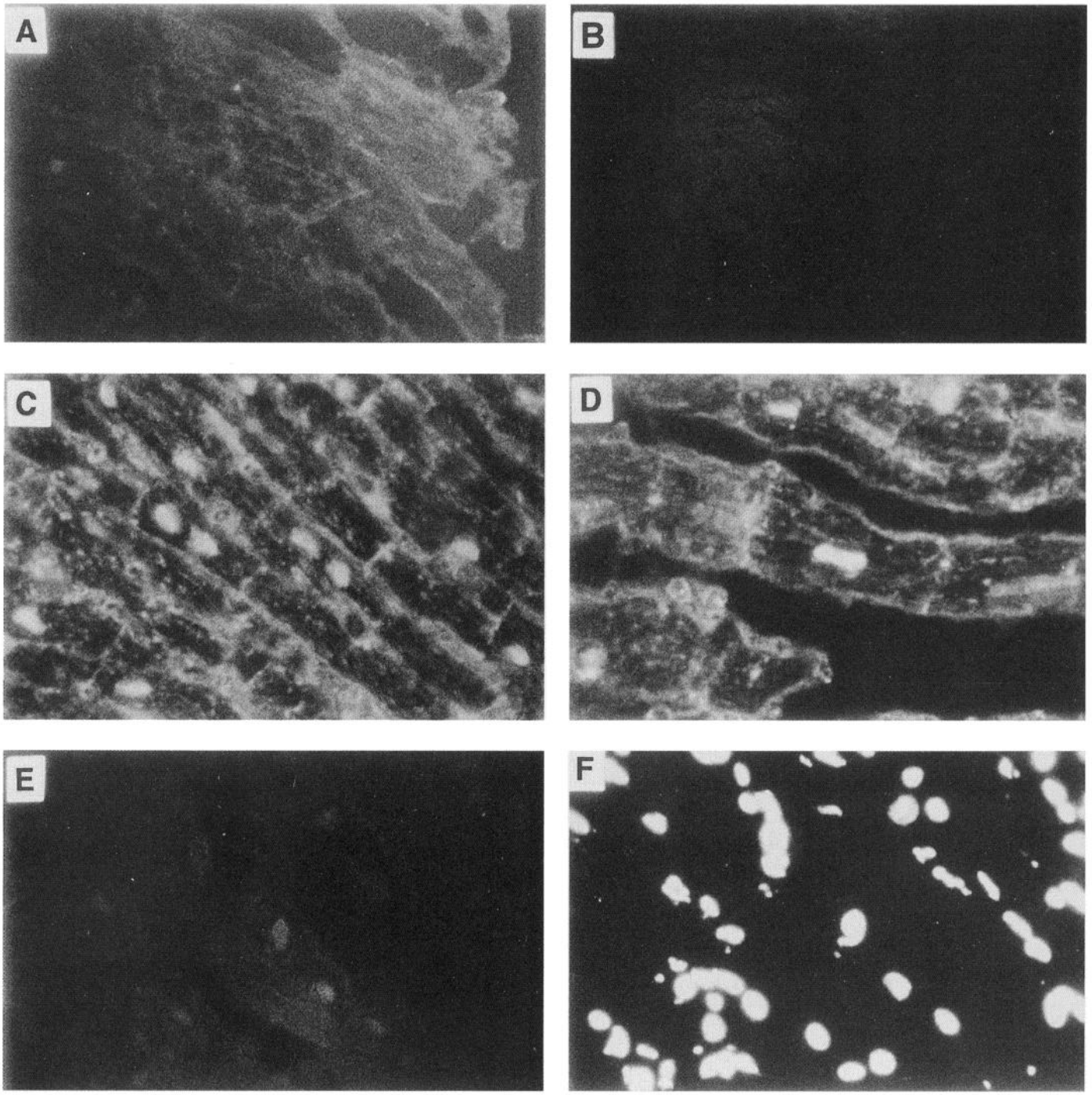

Fig. 7. Immunofluorescent detection of p27 protein on longitudinal sections from LV tissues of SH and AC rats at *day 14* postoperation. *A*: rabbit antibody to cardiac troponin I specifically stains the cytoplasm of myocytes and was detected by fluorescein isothiocyanate (FITC)-conjugated anti-rabbit immunoglobulin G (IgG). *B*: incubation of LV section from an SH rat heart with antibody to p27 after adsorption with the synthetic p27 peptide gives negative staining. *C* and *D*: double staining with antibody to cardiac troponin I and antibody to p27 detected with biotin-conjugated goat anti-rabbit IgG followed by streptavidin-Texas Red on LV sections from SH (*C*) and AC (*D*) rat heart shows nuclear localization of p27 in cardiomyocytes. *E* and *F*: section obtained from AC rat heart double stained with antibody to p27 and detected by FITC-conjugated anti-rabbit IgG (*E*) and with propidium iodide (*F*). Final magnification: ×600.

during the development of LVH in the rat. The importance of cell cycle-dependent molecules in modulating growth of myocardial tissue has been reported recently by Yoshizumi and colleagues (31). These authors demonstrated that, in human and rat cardiac tissue, downregulation of cyclins A and B (G_1/S and G_2/M phase cyclins) may contribute to the permanent withdrawal of cardiomyocytes from the cell cycle. Furthermore, we have reported recently that the protein expression and activities of certain cyclins and CDKs are downregulated

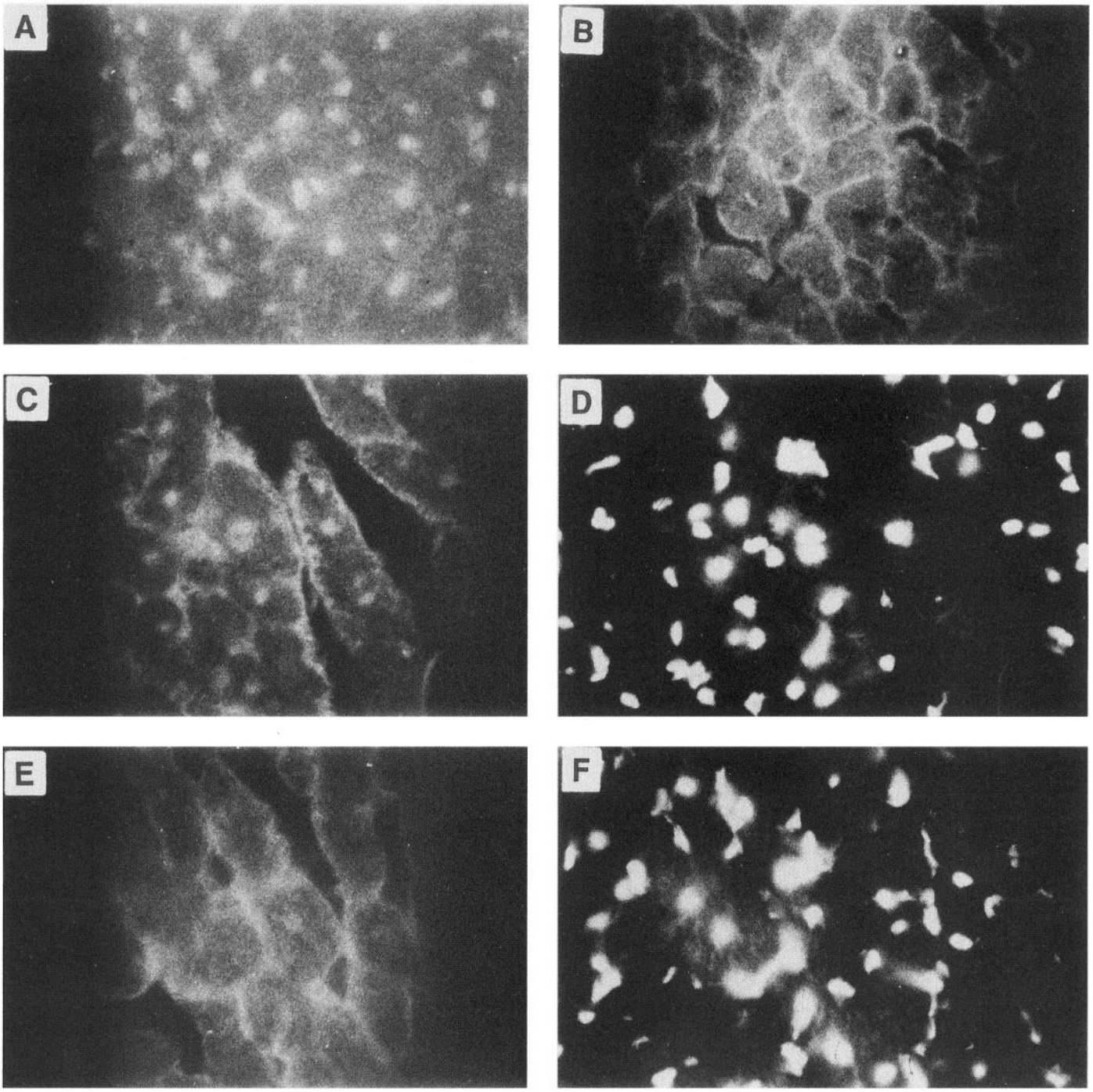

Fig. 8. Immunofluorescent detection of p21 protein on transverse sections from LV tissues of untreated, SH, and AC rats. *A*: antibody to p21-stained nuclei of cardiomyocytes in untreated rat LV tissue was detected by FITC-conjugated anti-rabbit IgG. *B*: antibody to laminin on the sequential section shown in *A* stained myocyte membranes. *C-F*: triple staining using an antibody to laminin to outline cardiomyocytes demonstrates T tubules (*C* and *E*), propidium iodide to label nuclei (*D* and *F*), and an antibody to p21 (*C* and *E*) on sections from SH (*C* and *D*) and AC (*E* and *F*) rats at *day 14* postoperation. Final magnification: ×600.

during normal cardiomyocyte development, whereas the expression of certain CDKI molecules is upregulated (5, 25), and this may help to explain why >95% of adult cardiomyocytes are known to exist in the G_0/G_1 phase of the cell cycle (18). In addition, Kiyokawa and colleagues (15) recently have shown that knockout mice lacking the CDKI molecule p27 displayed an increase in the size of a variety of organs, including the heart, thus directly implicating this molecule in modulating heart size. Despite the evidence suggesting that cyclins, CDKs, and CDKIs are involved in normal cardiac growth, no data are available to show how the expression of cell cycle molecules changes during the development of LVH. In this study, we have shown, by a

combination of RT-PCR, immunoblotting, and immunocytochemistry, that the mRNA and protein expression of p21 and p27 are downregulated significantly during the development of pressure overload-induced LVH and that this downregulation occurs primarily in the nuclei of cardiomyocytes. That LVH had indeed occurred in our model was demonstrated by a 50% increase in LV weight-to-body weight ratio in AC rats compared with SH control animals by 21 days after operation (Fig. 2). Consistent with this finding, we also were able to show by immunocytochemistry a significant increase in myocyte cell size 14 days after AC (Fig. 7, *C* and *D*). Our results suggest that downregulation of p21 and p27 in LV tissue may play a role in the changes in growth potential that occur in cardiac myocytes during pressure overload-induced LVH. Interestingly, the downregulation of p21 and p27 in myocytes was only seen during a relatively short period in our model of LVH. Thus, 2 wk after the AC operation, the initial decrease in p21 and p27 mRNA in LV tissue of AC rats was followed by a subsequent increase in mRNA expression such that levels were not significantly different from SH levels. Similar changes were observed for expression of p21 and p27 proteins, although the time frame for downregulation was more prolonged than for mRNA levels. These results are consistent with the fact that downregulation of p21 and p27 during the development of LVH probably is regulated at the level of mRNA transcription. The alterations in p21 and p27 mRNA and protein levels were consistent with our observation that LV mass in AC rats increased predominantly during the first 2–3 wk after operation because no subsequent increases in LV mass were seen during the 3- to 6-wk period after operation (Fig. 2*A*).

Interestingly, we observed that p27 protein expression did not mimic the expression pattern of p27 mRNA in SH rats. Thus p27 mRNA was expressed at a constant level throughout the 42-day postoperative period in SH rats, whereas p27 protein levels were low during the initial 1–14 days after operation but then increased progressively with time. The exact reason for this discrepancy between mRNA and protein expression remains unknown at this time, although our observations are consistent with a previous report by Hengst and Reed (13) that showed that p27 protein levels fluctuated during the cell cycle, whereas p27 mRNA levels remained unchanged, suggesting a translational control of p27 during the cell cycle. Indeed, it now is fairly well established that p27 expression is regulated at the posttranscriptional level (e.g., Ref. 10). It was interesting to note also that whereas p27 protein levels rose significantly in SH and AC animals during the 6-wk postoperative period, p21 protein levels remained constant in SH animals for the duration of the experiment. The precise reason for this rise in p27 remains unknown at this time, although a number of factors could be responsible. One possibility is that trauma experienced by SH and AC animals after operation causes changes in neural and/or humoral factors that may induce subsequent changes in specific gene and/or protein expression in the heart.

In summary, we have shown that expression of the CDKI molecules p21 and p27 alters dramatically, but transiently, during the development of LVH in the rat. The reason(s) why CDKI molecule expression becomes downregulated during the initial few weeks after the development of LVH or which factor(s) triggers the subsequent increase in p21 and p27 in cardiomyocytes after the initial period of downregulation during hypertrophy remains unknown at the present time. However, it is possible that the activity of certain cardiac muscle-specific transcriptional regulators may be involved in an analogous manner to the reported p53-independent induction of p21 by MyoD during terminal differentiation of skeletal muscle cells (10). Our hypothesis for why CDKI molecule expression decreases during the development of LVH is that an adjustment to the intracellular balance between the levels of positive (cyclins and CDKs) and negative (CDKIs) regulators of the cell cycle in cardiomyocytes is required to enable compensatory growth to occur. Thus if the levels of certain negative regulators were decreased, with or without a concomitant increase in the levels of certain positive regulators, then the cell could progress through G_1, thereby permitting increases in mRNA and protein synthesis that are necessary for hypertrophic growth (20). Once the levels of mRNA and protein syntheses had reached sufficient levels for adequate development of LVH, then the levels of CDKI molecules would increase, concomitant with a decrease in any elevated positive regulator expression, to those present before the induction of LVH leading to cell cycle arrest. Additional support for our hypothesis has been obtained recently in a parallel study to investigate changes in positive regulator expression during the development of LVH. Results from this additional study show that protein expression of certain CDKs (e.g., CDK4 and CDK6 but not CDC2) and cyclins (e.g., cyclins D_2 and D_3 but not cyclins D_1 or A) are upregulated concomitant with the decrease in p21 and p27 levels during the development of LVH (unpublished observations). A similar hypothesis has been proposed recently by Halevy and colleagues (10) for the maintenance of permanent cell cycle withdrawal in differentiated skeletal myocytes. These investigators have proposed that a positive feedback loop mechanism is involved in maintaining terminal differentiation such that MyoD is required to remain functionally active to ensure elevated p21 levels in these cells. Disruption of this pathway would result in a loss of p21 expression concomitant with an increase in the activities of various CDK-cyclin complexes leading to cell cycle progression.

It is possible that the discovery that downregulation of p21 and p27 correlates with the adaptive growth of cardiac myocytes during pressure overload-induced LVH in vivo may provide us with an opportunity to understand more clearly the mechanisms of this process and may eventually lead to successful strategies for the treatment of this disease.

We are grateful to Drs. M. Avkiran and Y. Shimada for surgical assistance in aortic constriction and D. J. Hearse for continued encouragement.

This work was supported by the Wellcome Trust (to J.-M. Li) and the British Heart Foundation (to G. Brooks).

Address for reprint requests: G. Brooks, Cardiovascular Research Group/Prolifix Ltd., 1–3 Burtonhole Lane, Mill Hill, London NW7 1AD, UK.

Received 21 October 1996; accepted in final form 29 April 1997.

REFERENCES

1. **Boheler, K. R., and K. Schwartz.** Gene expression in cardiac hypertrophy. *Trends Cardiovasc. Med.* 2: 176–182, 1992.
2. **Boluyt, M. O., L. O'Neill, A. L. Meredith, O. H. L. Bing, W. W. Brooks, C. H. Conrad, M. T. Crow, and E. G. Lakatta.** Alteration in cardiac gene expression during the transition from stable hypertrophy to heart failure. *Circ. Res.* 75: 23–32, 1994.
3. **Bradford, M. M.** A rapid and sensitive method for the quantitation of microgram quantities of protein utilizing the principle of protein-dye binding. *Anal. Biochem.* 72: 248–254, 1976.
4. **Brooks, G., M. W. Goss, J. A. East, and I. R. Hart.** Growth of melanocytic cells is associated with down-regulation of protein kinase C α, δ, and ϵ isoforms. *J. Biol. Chem.* 268: 23868–23875, 1993.
5. **Brooks, G., R. A. Poolman, C. J. McGill, and J.-M. Li.** Expression and activities of cyclins and cyclin-dependent kinases in developing rat ventricular myocytes. *J. Mol. Cell. Cardiol.* In press.
6. **Chevalier, B., F. C. Amrani, C. Heymes, and B. Swynghedauw.** Molecular basis of regression of cardiac hypertrophy. *Am. J. Cardiol.* 73: 10C–17C, 1994.
7. **Chien, K. R., K. U. Knowlton, H. Zhu, and S. Chien.** Regulation of cardiac gene expression during myocardial growth and hypertrophy: molecular studies of an adaptive physiologic response. *FASEB J.* 5: 3037–3046, 1991.
8. **El-Deiry, W. S., T. Tokino, V. E. Velculescu, D. B. Levy, R. Parsons, J. M. Trent, D. Lin, W. E. Mercer, K. W. Kinzler, and B. Vogelstein.** WAF1, a potential mediator of p53 tumor suppression. *Cell* 75: 817–825, 1993.
9. **Frohlich, E. D., C. Apstein, A. V. Chobanian, R. B. Devereux, H. P. Dustan, V. Dzau, F. Fauad-Tarazi, M. J. Horan, M. Marcus, B. Massie, M. A. Pfeffer, R. N. Re, E. J. Roccella, D. Savage, and C. Shub.** The heart in hypertension. *N. Engl. J. Med.* 327: 998–1008, 1992.
10. **Halevy, O., B. G. Novitch, D. B. Spicer, S. X. Skapek, J. Rhee, G. J. Hannon, D. Beach, and A. B. Lassar.** Correlation of terminal cell cycle arrest of skeletal muscle with induction of p21 by MyoD. *Science* 267: 1018–1021, 1995.
11. **Harper, J. W., G. R. Adami, N. Wei, K. Keyomarsi, and S. J. Elledge.** The p21 Cdk-interacting protein Cip1 is a potent inhibitor of G1 cyclin-dependent kinases. *Cell* 75: 805–816, 1993.
12. **Haworth, R. S., M. Yasutake, G. Brooks, and M. Avkiran.** Cardiac Na^+/H^+ exchanger during post-natal development in the rat: changes in mRNA expression and sarcolemmal activity. *J. Mol. Cell. Cardiol.* 29: 321–332, 1997.
13. **Hengst, L., and S. I. Reed.** Translational control of $p27^{Kip1}$ accumulation during the cell cycle. *Science* 271: 1861–1864, 1996.
14. **Izumo, S., B. Nadal-Ginard, and V. Mahdavi.** Protooncogene induction and reprogramming of cardiac gene expression produced by pressure overload. *Proc. Natl. Acad. Sci. USA* 85: 339–343, 1988.
15. **Kiyokawa, H., R. D. Kineman, K. O. Manova-Todorova, V. C. Soares, E. S. Hoffman, M. Ono, D. Khanam, A. C. Hayday, L. A. Frohman, and A. Koff.** Enhanced growth of mice lacking the cyclin dependent kinase inhibitor function of $p27^{Kip1}$. *Cell* 85: 721–732, 1996.
16. **Levy, B. L., M. Avkiran, R. Ferrari, and D. J Hearse.** Impaired skeletal muscle fatigue resistance in rats with pressure overload-induced left ventricular hypertrophy. *J. Mol. Cell. Cardiol.* 28: 183–195, 1996.
17. **Li, J.-M., A. C. Horsfall, and R. N. Maini.** Anti-La (SS-B) but not anti-Ro52 (SS-A) antibodies cross-react with laminin—a role in the pathogenesis of congenital heart block? *Clin. Exp. Immunol.* 99: 316–324, 1995.
18. **McGill, C. J., and G. Brooks.** Cell cycle control mechanisms and their role in cardiac growth. *Cardiovasc. Res.* 30: 557–569, 1995.
19. **Morgan, D. O.** Principles of CDK regulation. *Nature* 374: 131–134, 1995.
20. **Morgan, H. E., E. E. Gordon, Y. Kira, B. H. L. Chua, L. A. Russo, C. J. Peterson, P. J. McDermott, and P. A. Watson.** Biochemical mechanisms of cardiac hypertrophy. *Annu. Rev. Physiol.* 49: 533–543, 1987.
21. **Noda, A., Y. Ning, S. F. Venable, O. M. Pereira-Smith, and J. R. Smith.** Cloning of senescent cell-derived inhibitors of DNA synthesis using an expression screen. *Exp. Cell Res.* 211: 90–98, 1994.
22. **Norbury, C., and P. Nurse.** Animal cell cycles and their control. *Annu. Rev. Biochem.* 61: 441–470, 1992.
23. **Pausson, M., and K. Saladin.** Mouse heart laminin. *J. Biol. Chem.* 264: 18726–18732, 1989.
24. **Polyak, K., J. Kato, M. J. Solomon, C. J. Sherr, J. Massague, J. M. Roberts, and A. Koff.** $p27^{Kip1}$, a cyclin-Cdk inhibitor, links transforming growth factor-β and contact inhibition to cell cycle arrest. *Genes Dev.* 8: 9–22, 1994.
25. **Poolman, R. A., and G. Brooks.** Expression of the Cip/Kip family of the cyclin dependent kinase inhibitors during cardiac development (Abstract). *Circulation.* 94: I-157, 1996.
26. **Price, R. L., M. Nakagawa, L. Terracio, and T. K. Borg.** Ultrastructural localization of laminin on in vivo embryonic, neonatal and adult rat cardiac myocytes and in early rat embryos raised in whole-embryo culture. *J. Histochem. Cytochem.* 40: 1373–1381, 1992.
27. **Toyoshima, H., and T. Hunter.** p27, a novel inhibitor of G1 cyclin-Cdk protein kinase activity, is related to p21. *Cell* 78: 67–74, 1994.
28. **Waga, S., G. J. Hannon, D. Beach, and B. Stillman.** The p21 inhibitor of cyclin-dependent kinases controls DNA replication by interaction with PCNA. *Nature* 369: 574–578, 1994.
29. **Weber, K. T., and C. G. Brilla.** Pathological hypertrophy and cardiac interstitium. *Circulation* 83: 1849–1865, 1991.
30. **Xiong, Y., G. J. Hannon, H. Zhang, D. Casso, R. Kobayashi, and D. Beach.** p21 is a universal inhibitor of cyclin kinases. *Nature* 366: 701–704, 1993.
31. **Yoshizumi, M., W.-S. Lee, C.-M. Hsieh, J.-C. Tsai, J. Li, M. A. Perrella, C. Patterson, W. O. Endege, R. Schlegel, and M.-E. Lee.** Disappearance of cyclin A correlates with permanent withdrawal of cardiomyocytes from the cell cycle in human and rat hearts. *J. Clin. Invest.* 95: 2275–2280, 1995.